Wideband and polarization-independent silicon waveguide to plasmonic waveguide mode converter based on optimization algorithms

Liu, Zunwei, Zhang, Tian, Dai, Jian, Xu, Kun

Zunwei Liu, Tian Zhang, Jian Dai, Kun Xu, "Wideband and polarization-independent silicon waveguide to plasmonic waveguide mode converter based on optimization algorithms," Proc. SPIE 11455, Sixth Symposium on Novel Optoelectronic Detection Technology and Applications, 114554J (17 April 2020); doi: 10.1117/12.2564976

Event: Sixth Symposium on Novel Photoelectronic Detection Technology and Application, 2019, Beijing, China

Wideband and polarization-independent silicon waveguide to plasmonic waveguide mode converter based on optimization algorithms

Zunwei Liu[a], Tian Zhang*[a], Jian Dai[a], and Kun Xu[a]

[a]State Key Laboratory of Information Photonics and Optical Communications, Beijing University of Posts and Telecommunications, Beijing, P.R. China 100876

ABSTRACT

Conventional silicon optical waveguide can be effectively coupled to plasmonic waveguide, but there is no structure of comparable coupling efficiency, wide optical bandwidth and polarization independence to convert light from silicon waveguide to metal-dielectric-metal (MDM) waveguide. In this paper, we investigate a novel mode converter based on the embedded coding metamaterials to effectively convert the TE/TM mode in a silicon waveguide to the SPPs mode. We use some optimization methods (genetic algorithm, particle swarm optimization, multi-traversal direct-binary search and simulated annealing) in the design of coding metamaterials to improve the performance metrics. In order to obtain better results, we change the value of different parameters under the control of a single variable to study its influence on the structure of the design. The simulation results have been demonstrated numerically that high transmission efficiency is up to 93% and the bandwidth can cover from 1450 nm to 1650 nm, the converter can perform polarization-invariant conversion as well. Compared with the previous researches, we not only propose a high-performance mode converter but also introduce an efficient algorithm for the inverse design of coding metamaterials.

Keywords: Mode converter, optimization algorithms, inverse design, plasmonics, embedded coding metamaterials

1. INTRODUCTION

Surface plasmon polaritons (SPPs) is an electromagnetic wave in the infrared or visible light band that propagates on the metal-dielectric or metal-air interface.[1-2] Owing to breaking the limit of diffraction, Plasma waveguides have potential in constructing ultra-compact photonic devices and greatly enhancing light-matter interactions. It has been proven that many applications of optical devices are based on plasma waveguides, such as plasmonic filter,[3] splitter,[4] switch,[5] modulator,[6] absorber,[7] sensor,[8] logic gate,[9] and so on. Recently, there are many studies[10-14] related to the plasma mode converter (PMC), as an important optical device in the optical interconnection system, PMC can effectively convert TE/TM mode light in a silicon waveguide to the SPPs mode in a plasmonic waveguide. In recent years, in order to meet the needs of different integrated environments, various plasmonic waveguide structures, such as metal-dielectric-metal (MDM) waveguide, metal-insulator-metal (MIM) waveguide, metal groove and metallic slot waveguide have been used to design PMC.[10] For different PMC structures, conversion efficiency and conversion bandwidth are two very essential performance parameters. For example, the PMCs proposed in earlier research articles have a conversion efficiency of more than 85%, operating 1 dB bandwidth in the range of 200 nm.[11] In order to ensure constant total conversion efficiency and preserve the incident polarization information, a tunable directional coupler with polarization control is designed.[12] Two new structures have been proposed to improve the conversion efficiency of silicon waveguides to MIM waveguides, the traditional straight waveguide in the PMC was replaced with a slot-taper structure for gradually squeezing the TE / TM mode from the silicon waveguide into the plasmonic waveguide.[13] In addition to the clever design of the device structure, some optimization methods were also used to find the appropriate groove-cone structure parameters.[14] However, the optimization abilities were limited because it only optimized for a specific taper structure rather than a relatively complete optimization space. And there were few polarization-invariant PMC had high conversion efficiency and wide bandwidth simultaneously. It's expected to further improve conversion efficiency and bandwidth by designing ingenious device structure and selecting effective optimization algorithms.

In the current researches, gradient based methods, gradient free methods, and model based methods can be used to design and optimize photonic devices.[15-16] The adjoint variable method (AVM) is a kind of gradient based algorithm.

*ztian@bupt.edu.cn

Sixth Symposium on Novel Optoelectronic Detection Technology and Applications, edited by Junhao Chu, Huilin Jiang
Proc. of SPIE Vol. 11455, 114554J · © 2020 SPIE · CCC code: 0277-786X/20/$21 · doi: 10.1117/12.2564976

These algorithms can be used to design linear as well as nonlinear photonic devices, which need to calculate the gradient of the objective function according to the physical background.[17] Artificial neural networks and random forests belong to model-based methods, which can reversely design photonic devices.[16, 18] Generally, we set some physical parameters on the input side and get electromagnetic response on the output side. However, these methods require a relatively long time to train data.[16] Compared with gradient based and model based methods, gradient free methods based on search strategies and evolutionary algorithms are simple and effective.[15] Genetic algorithm (GA) and particle swarm algorithm (PSO) are two kinds of evolutionary algorithms, which are related to biological evolution and natural selection.[15] It should be noted that the convergent speed of the evolutionary algorithm are relatively slow because they need to control the population consisted of individuals. Simulated annealing algorithm (SA) and direct-binary search algorithm (DBS) are search algorithms, which are simple and the convergence time is short as well.[19] But the finite traversal times (usually only once) restrict the optimization ability of the DBS.

In our paper, we propose a new mode converter based on embedded coding metamaterials. We use the algorithm to reversely design the PMC structure, and through FDTD simulation, we finally get the best PMC optimized by multi-traversal DBS, which can achieve high conversion efficiency and wide bandwidth.

2. DEVICE DESIGN

As shown in Fig.1, we propose a PMC that consists of a silicon waveguide, a silicon-based coding metamaterial (SCM), and a plasmonic MDM waveguide. The thickness of the underlying silicon substrate is 3μm, and all waveguides and SCMs are placed on it. The SCM whose footprint is 1×1 μm^2, is consists of M×N square pixels. It connects the silicon waveguide with the MDM waveguide and embedded into the metal (Au). There are two fill modes for each pixel in the SCM. The silicon fill corresponds to the value "1", and the air fill corresponds to the value "0". The input light in TM / TE mode is transferred through SCM to SPPs mode in MDM waveguide. Obviously, the SCM provides a relatively broad optimization space compared with the specific device structure in Ref. 14. The length, width, and height of the silicon waveguide are 3 μm, 0.4 μm and 0.25 μm, respectively. What's more, the length, width, and height of the MDM waveguide are 3 μm, 3 μm, and 0.25 μm, respectively.

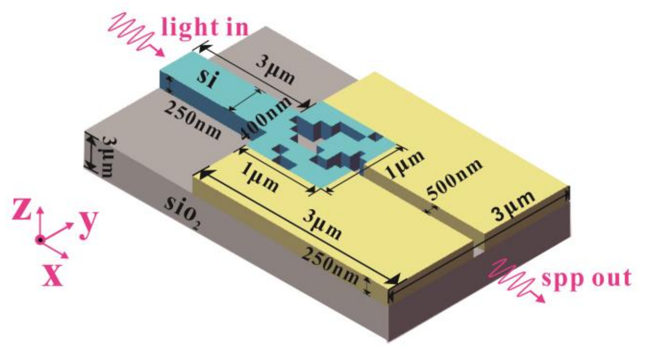

Fig.1 Structure schematic of the proposed PMC.

In our simulation, the transmission spectrum of the PMC is calculated by the 2.5-dimensional finite-difference time-domain (FDTD) method (adopting Lumerical MODE Solutions). The metal in the FDTD simulation is modeled by the Drude model with (ε_∞, ω_p, γ_p) = (3.7, 9.1 eV, 0.018 eV).[16] The conversion efficiency of PMC is defined as the ratio of the power coupled into the plasmonic waveguide and the output power of the silicon waveguide. It should be noticed that the transmission loss of the MDM waveguide is calculated by placing several monitors in the waveguide.

3. OPTIMIZATION ALGORITHMS

In our article, four algorithms are used to design and optimize the PMC structure, which are GA, PSO, SA and DBS algorithms. Among these four algorithms, GA and PSO belong to evolutionary algorithms, and SA is the search algorithm. As typical gradient free methods, GA and PSO have been applied in optimizing for various photonics devices because of their simplicity and effectiveness.[15]

3.1 Genetic algorithm

We use genetic algorithm to design the PMC structure firstly. The detail steps are as follows: (i) The population individual is set to N = 50, and the first generation of the population with a value of "0" or "1" is randomly generated. The elements in the matrix of each individual correspond to the pixels in the PMC. (ii) For each of the N individuals, we calculate its transmission spectrum (using the FDTD method). We define the value of target transmission spectrum to "1" in the wavelength range of 1.5 μm to 1.6 μm. The fitness function is defined as the difference between the target transmission spectrum and the actual transmission spectrum. Obviously, the smaller the difference between the two spectrums, the higher the fitness of the corresponding individual can get. (iii) Trying to generate a new population by using the selection, crossover and mutation procedures. We set the roulette-wheel selection with gap selection ratio 0.8 to select two parent individuals from previous generation in the selection process.[16] Here, the SCMs with smaller difference are selected with higher probability. In the crossover process, the selected SCMs cross over to generate a new SCM based on the uniform crossover method with a crossover probability of 0.3. In the mutation process, we set mutation probability to 5%, meaning that each pixel in the SCM has 5% probability to flip from 0 to 1 or 1 to 0. (iv) The newly generated SCMs are evaluated to determine the GA whether to stop or not. If the genetic generation reaches to 100 or the difference remain unchanged for more than 5 times, then GA stops, otherwise, proceeds to Step (ii).

3.2 Particle swarm optimization

As another evolutionary algorithm, particle swarm optimization is more suitable for decimal system, while genetic algorithm is more suitable for binary system.[20] Each particle in a particle swarm represents a possible solution to a problem. The individuals (SCMs) in a population depend on the globally optimal individual and historically optimal record to search for optimal solution.[20] Here, it should be noticed that we use the discrete binary PSO (DBPSO) rather than the standard PSO in the paper. The algorithm rules of DBPSO and PSO are the same, but the only difference is that the velocity of the standard PSO directly affects the position of particle, while that of DBPSO is converted to a flip probability based on the sigmoid function.[21] The change of the pixels in SCMs depend on these flip probability determines.

The details of the algorithm are as follows: (i) We set the number of particles to 50 and initialize the particle swarm randomly. (ii) The fitness function is defined as the difference between the transmission spectrum of the particle and the target transmission spectrum whose value is 1. Then we calculate the fitness in the individual (SCMs) in the population. (iii) We update the particle's speed and turnover results according to the fitness. (iv) Evaluating the updated SCMs and stop the algorithm if it has been iterated 200 times or the difference remains more than 5 times unchanged. The speed range, inertia weight and acceleration constants of the DBPSO in this article are set as -1~1, 1, and c_1=c_2=1.49, respectively.

3.3 Simulated annealing algorithm

The simulated annealing algorithm is a general probability algorithm used to find the optimal solution of a proposition in a large search space. It is a random optimization algorithm based on Monte-Carlo iterative solution strategy, which utilizes the similarity between the annealing process of solid matter in physics and general combinatorial optimization problems.[19] The SA algorithm sets a higher initial temperature, randomly finds the global optimal solution of the objective function, and accepts worse solutions than the current one to a certain extent . As the temperature continues declining, the degree of accepting poor solutions in SA become less and less. This makes the SA algorithm avoid the local optimal situation. In each iteration, we use the FDTD algorithm to randomly generate a set of values and evaluate the transmission spectrum of the SCM, then calculate the difference from the target transmission spectrum to determine whether the newly generated PMC is accepted. Here, it's should be noticed that the acceptance probability is determined by the Metropolis standard.[22] In our simulation, the maximum and minimum temperatures of SA were set to 2000 and 1e-18, respectively.

3.4 Direct-binary search algorithm

The DBS algorithm is a non-linear search algorithm. DBS not only has a simple algorithm principle but also can achieve relative better simulation results. The specific algorithm steps of DBS are as follows: (i) The SCM is numerically initialized with value of "0" or "1" randomly, which is assigned to the PMC. Then the transmission spectrum value of the PMC is calculated by utilizing the FDTD method. (ii) The value of a pixel at a certain position in the SCM is flipped. If the previous value of a pixel at that location is 0, then flip it to 1, and vice versa. Here, it should be noted that the pixel value change is performed in order. The pixel in the first row and the first column is flipped firstly, then pixel in the first row and the second column in flipped, and so on until the pixels in the first row are completely turned. We use the same rule to regulate the second row until all rows and columns are flipped. Then, we use FDTD method to calculate the transmission spectrum of the newly generated SCM included in PMC. The sum of the newly generated transmission spectrum is compared with the sum of the transmission amounts before the pixels are not inverted. If the sum of the transmission amount of the newly generated transmission spectrum is greater than the previous, the overturned value of pixel is accepted. Otherwise, the original value of the pixel is kept unchanged. (iii) The condition of DBS is evaluated to determine the method whether to stop or not. In the traditional DBS, if the algorithm traverses all pixels in SCM once, then it stops, otherwise, proceeds to Step (ii). In order to further improve the algorithm searching ability, we propose a multi-traversal DBS (MDBS) to traverse SCM several times in succession. And we use the MDBS to optimize the SCM in PMC.

4. SIMULATION RESULTS

For SCM with 40 × 40 pixels, we use genetic algorithm, DBPSO algorithm and SA algorithm to optimize PMC. The simulation results are shown in Fig.2. Fig.2 (a) is the transmission spectrum curve of PMC without algorithm optimization. The initial value of SCM is randomly generated. It can be seen in this figure that in the wavelength range of 1.50 μm to 1.60 μm, the transmission spectrum values are very low. The maximum value of the transmission spectrum is less than 0.3, which is almost impossible to effectively transmit light between the two waveguides. Fig.2 (b) shows the variation of differences for GA and DBPSO in different iterations within 200 iterations. Fig.2 (c) shows the difference changes of SA algorithm within 2500 iterations. It can be seen from Fig.2 (b) (c) that the three curves have the same trend, and the difference value is smaller and smaller with the increase of iterations. It can be found that the differences of GA, DBPSO and SA decrease from 83.2, 72.5, and 75.6 to 32.3, 35.7 and 27, respectively. And in the last iteration, the average absolute deviation for each point in the transmission spectrum are 32.3/100=0.323 (GA), 35.7/100=0.357 (DBPSO) and 27/100=0.27 (SA). Obviously we can draw this conclusion from the figure: all three algorithms are effective (convergent), because the difference decreases and the final value is small. What's more the optimized transmission spectrum is close to the target transmission spectrum. Fig.2 (d) is the final transmission spectrum curve optimized by the three algorithms. It can be seen from the figure that the values of the best transmission spectrum are all above 50%, and the maximum transmittances of GA, DPSPSO, and SA are 0.75, 0.71 and 0.78 respectively. Obviously, the PMC transmission spectrum has been significantly improved after the algorithm optimization.

For GA and DBPSO, we also considered the impact of setting different parameter values on the optimization results. In order to ensure the accuracy of the results and make the research more rigorous, we only change the value of one variable at a time with the controlled variable method. Fig.3 (a) shows the effects of different population sizes (PS), genetic algorithm's crossover probabilities (CP), and mutation probabilities (MP) on the PMC optimization results in the genetic algorithm. It shows the tendency of changes about differences of different parameter groups within 100 iterations. It can be found that the fitness decreases from 33.7 to 33.0 when the population size increases from 60 to 100, indicating that the larger the population size is, the better the optimization result is. The larger the population is, the stronger the global search capability can get, which lead to the better the final optimization result [16]. For the mutation probabilities, a larger value will result in worse algorithm stability and lower convergence speed. Fig.3 (b) shows the optimized PMC transmission spectrum values for different parameter groups. It can be seen from the figure that a larger population and a smaller probability of mutation can improve the optimization result. Similarly, Fig.3(c) exhibits the variation of differences for different velocity ranges (V_{min} ~V_{max}) and inertia weights (w) of DBPSO. It can be found that the difference decreases from 55.9 to 35.7 when the inertia weight increases from 0.8 to 1. We find that the relationship between speed range and difference is not linear. Generally, inertia weights and speed range of each iteration will affect the decay speed and search range, then further affect the convergence speed of the algorithm. Due to the fast attenuation speed of DBPSO, the optimization effect become worse when the inertia weight get reduced. Corresponding to the above conclusion, Fig.3 (d) shows the value of the PMC transmission spectrum after 200 iterations optimization under different inertia weights and speed range. In order to achieve rapid convergence, the variable inertia weight for different iterations can be employed in DBPSO. And the velocity range should be configured in a reasonable range to control the relationship between the convergence speed and search scope.

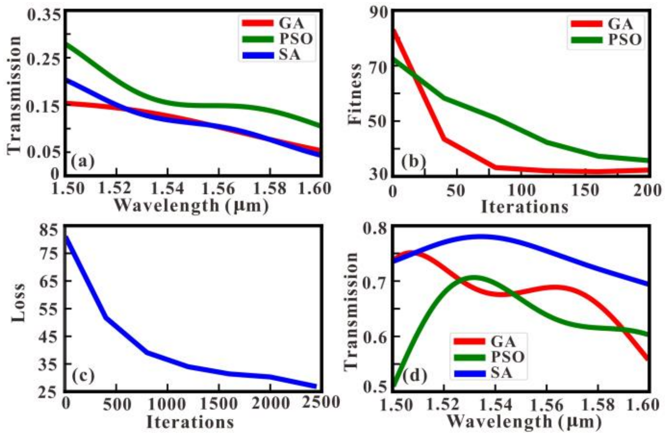

Fig.2 (a) The transmission spectrums of the PMCs whose SCMs are randomly initialized for GA, DBPSO and SA. (b) The variation of differences for GA and DBPSO in different iterations. (c) The variation of differences for SA in different iterations. (d) The simulated transmission spectrums after GA, DBPSO and SA optimizations.

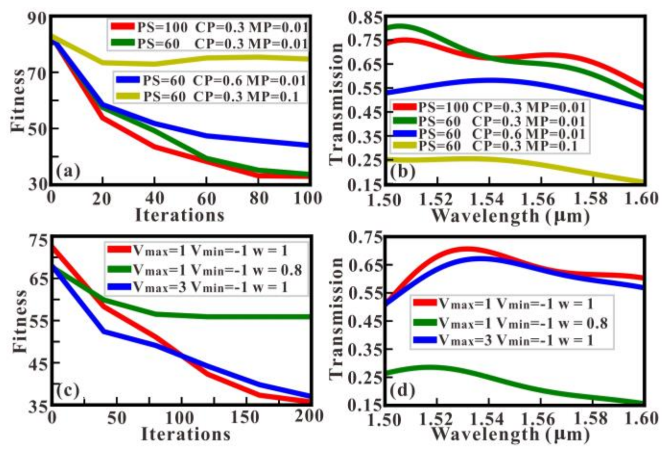

Fig.3 (a) The variation of differences for the GA with different optimization parameters. (b) After the optimization, the simulated transmission spectrums for different parameters of GA. (c) The variation of differences for DBPSO with different optimization parameters. (d) After the DBPSO optimization, the simulated transmission spectrums for different optimization parameters.

Finally, we use MDBS to optimize PMC with three densities of 20×20, 30×30 and 40×40. As shown in Fig.4 (a), there are three initial transmission spectrum curves of PMC without MDBS algorithm optimization. It can be clearly seen from the figure that the maximum values of the transmission spectra of the three densities are all less than 0.2, which indicates that the randomly initialized PMC can hardly effectively convert light from the silicon waveguide to the MDM waveguide. We use the MDBS algorithm to optimize PMC for 5 traversals, as shown in Fig.4 (b), which is the difference curve between the optimized transmission spectrum and the target transmission spectrum after each iteration. Obviously, the curve trend in the figure drops sharply, indicating that the MDBS algorithm is effective. The simulation data shows that the optimization results which obtained after the first traversal are close to the results optimized by the GA, DBPSO, and SA algorithms previously. We continue performing four traversals of SCM with three densities by using MDBS, it can be seen that the difference between the transmission spectrum of the PMC and the target transmission spectrum gradually decreases as the iterations increases. After five traversals, the average absolute deviation for each point in transmission spectrums are $5.73/100 \approx 0.057$, $5.79/100 \approx 0.06$ and $12.08/100 \approx 0.12$ for the SCMs with 40×40, 30×30 and 20×20, respectively. Obviously, the transmission spectrums of the PMCs optimized by the MDBS are closer to the targeted transmission spectrum than the optimized results by using GA, DBPSO and SA, therefore, effect of MDBS algorithm optimization is the best. The final PMC transmission spectrum curve obtained after five traversals is shown in Fig.4 (c), where SCMs with the density of 40 × 40 and 30 × 30 possess a high transmittance in the wavelength range of 1.45 μm ~ 1.65 μm. Both of transmission spectrums can reach above 0.94, implying that PMC with high conversion efficiency is achieved.

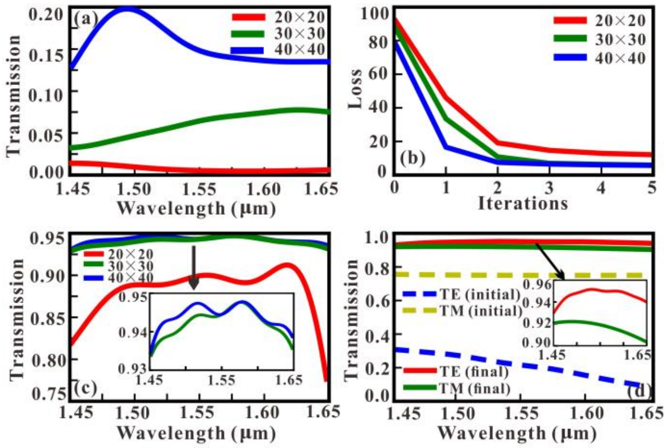

Fig.4 (a) The transmission spectrums of the PMCs whose SCMs are randomly initialized for different densities. (b) The variation of differences for different traversal times. (c) The optimized transmission spectrums for the SCMs with different densities after the fifth traversal. (d) The transmission spectrums of the PMC before the optimization (dash line) and after the optimization (solid line).

We use MDBS to optimize the SCM in five times, and through FDTD simulation, we finally design a PMC with high conversion efficiency and wide bandwidth. Compared with PMC for TM mode only, we have also designed a PMC that has high conversion efficiency in both TE mode and TM mode. Therefore, we need to modify the optimization target. The objective function is no longer the difference between the optimized transmission spectrum and the target transmission spectrum. We need to consider both TE mode and TM mode. In each iteration of MDBS, the FDTD simulation for PMC will be calculated twice: the first FDTD simulation is calculated for TM mode, and the second FDTD simulation is calculated for TE mode. Then, the differences between the targeted transmission spectrum and optimized transmission spectrum for TM mode and TE mode are added to comprehensively evaluate the performance of optimized SCM. If this value is reduced, the new SCM will be accepted, otherwise, it will be rejected. Fig.4 (d) shows the PMC transmission spectrum curve before the optimization (dotted line) and after optimization (solid line) of the MDBS algorithm. Obviously, the randomly initialized PMC cannot effectively convert the TM / TE mode in the silicon waveguide into the SPPs mode in the MDM waveguide. Surprisingly, after optimization by the MDBS algorithm, the conversion rates of both the TE mode and the TM mode have been improved. In the wavelength range of 1.45 μm to 1.65 μm, PMC transmission efficiency reaches 0.93 or more for TE mode and 0.91 or more for TM mode, suggesting a polarization-invariant PMC is achieved by optimizing for SCM based on the MDBS.

5. CONCLUSION

In summary, we have designed a new PMC that can be effectively implemented to convert the TE / TM mode in a silicon waveguide to the SPPs mode in a plasma waveguide. At the same time, we propose an effective SCM reverse design algorithm. We use GA, DBPSO, SA, and MDBS to optimize the SCM in PMC. Simulation results show that the PMC designed by the MDBS algorithm can achieve the best results, which can perform polarization-invariant conversion, and the conversion efficiency and bandwidth reach more than 0.93 and 200 nm, respectively. Compared with previous studies, the PMC designed in our paper has great advantages in conversion efficiency and bandwidth.

REFERENCES

[1] Gramotnev, D. K. and Bozhevolnyi, S. I., "Plasmonics beyond the diffraction limit," Nat. Photonics 4, 83-91 (2010).

[2] Zhang, T., Chen, L. and Li, X., "Graphene-based tunable broadband hyperlens for far-field subdiffraction imaging at mid-infrared frequencies," Opt. Express 21, 20888-20899 (2013).

[3] Li, H. J., Wang, L. L., Liu, J. Q., Huang, Z. R., Sun, B., and Zhai, X., "Investigation of the graphene based planar plasmonic filters," Appl. Phys. Lett. 103, 211104 (2013).

[4] Zhang, T., Yin, X., Chen, L. and Chen, X., "Ultra-compact polarization beam splitter utilizing a graphene-based asymmetrical directional coupler," Opt. Lett. 41(2), 356-359 (2016).

[5] Chang, W. S., Lassiter, J. B., Swanglap, P., Sobhani, H., Khatua, S. and Nordlander, P., "A plasmonic fano switch," Nano Lett. 12(9), 4977-4982 (2012).

[6] Melikyan, A. and et al, "High-speed plasmonic phase modulators," Nat. Photonics 8, 229-233 (2014).

[7] Xiong, X., Zou, C. L., Ren, X. F., and Guo, G. C., "Broadband plasmonic absorber for photonic integrated circuits," IEEE Photon. Techno. Lett. 26(17), 1726-1729 (2014).

[8] Rodrigo, D., Limaj, O., Janner, D., Etezadi, D. and et al, "Mid-infrared plasmonic biosensing with graphene," Science 349(6244), 165-168 (2015).

[9] Zhang, T., Zhou, J., Dai, J., Dai, Y., Han, X. and Li, J., "Plasmon induced absorption in a graphene-based nanoribbon waveguide system and its applications in logic gate and sensor," J. Phys. D: Appl. Phys. 51, 055103 (2018).

[10] Fang, Y. and Sun, M., "Nanoplasmonic waveguides: towards applications in integrated nanophotonic circuits," Light-Sci Appl. 4, e294 (2015).

[11] Melikyan, A., Kohl, M., Sommer, M., Koos, C., Freude, W. and Leuthold, J., "Photonic-to-plasmonic mode converter," Opt. Lett., 39(12), 3488 (2014).

[12] Lin, J., Mueller, J. P. B., Wang, Q., Yuan, G., Antoniou, N. and Yuan, X. C., "Polarization-controlled tunable directional coupling of surface plasmon polaritons," Science, 340(6130), 331-334 (2013).

[13] Zhu, B. and Tsang, H. K., "High coupling efficiency silicon waveguide to metal–insulator–metal waveguide mode converter," Journal of Lightwave Technology, 34(10), 2467-2472 (2016).

[14] Chen, C. and et al, "Design of highly efficient hybrid Si-Au taper for dielectric strip waveguide to plasmonic slot waveguide mode converter," Journal of Lightwave Technology, 33(2), 535-540 (2015).

[15] Molesky, S., Lin, Z., Piggott, A. Y., Jin, W., Vucković, Jelena, and Rodriguez, A. W., "Inverse design in nanophotonics," Nat. Photonics 12, 659-670 (2018).

[16] Zhang, T., Wang, J., Liu, Q., Zhou, J., Dai, J. and Han, X., "Efficient spectrum prediction and inverse design for plasmonic waveguide systems based on artificial neural networks," Photonics Research 7(3), 368-380 (2019).

[17] Hughes, T. W., Minkov, M., Williamson, I. A. D., and Fan, S., "Adjoint method and inverse design for nonlinear nanophotonic devices," ACS Photonics 5, 4781-4787 (2018).

[18] Zhang, T., Liu, Q., Dan, Y., Yu, S., Dai, J., and Han, X., "Inverse design and optimization of graphene metamaterial for multi-peak plasmon induced transparency based on machine learning and evolutionary algorithms," arXiv:1908.01354 (2019).

[19] Shen, B., Wang, P., Polson, R., & Menon, R., "An integrated-nanophotonics polarization beamsplitter with 2.4×2.4 μm2 footprint," Nat. Photonics 9, 378-382 (2015).

[20] Zhang, T., Wang, J., Dan, Y., Lanqiu, Y., Dai, J. and Han, X., "Efficient training and design of photonic neural network through neuroevolution," arXiv:1908.08012 (2019).

[21] Chuang, L. Y., Chang, H. W., Tu, C. J. and Yang, C. H., "Improved binary PSO for feature selection using gene expression data," Comput. Biol. Chem. 32(1), 29-38 (2008).

[22] Kirkpatrick, S. and et al, "Optimization by Simulated Annealing," Science 220(4598), 671-680 (1983).